Am. J. Hum. Genet. 58:743–748, 1996

The Locus for a Novel Syndromic Form of Neuronal Intestinal Pseudoobstruction Maps to Xq28

Alberto Auricchio,[1,2] Valeria Brancolini,[3] Giorgio Casari,[1] Peter J. Milla,[4] Virpi V. Smith,[4] Marcella Devoto,[3] and Andrea Ballabio[1,5]

[1]Telethon Institute of Genetics and Medicine, San Raffaele Biomedical Science Park, Milan; [2]Department of Pediatrics, "Federico II" University, Naples; [3]Department of Psychiatry, Columbia University, New York; [4]Gastroenterology Unit, Hospital for Sick Children, London; and [5]Department of Molecular Biology, University of Siena, Siena

Summary

The neuronal type of primary chronic idiopathic intestinal pseudoobstruction (CIIP) results from the developmental failure of enteric neurons to migrate or differentiate correctly. This leads to intestinal motility disorders, which are characterized by symptoms and signs of bowel obstruction in the absence of a mechanical obstacle. Most of these conditions are congenital, and among them some are inherited. One syndromic condition characterized by intestinal pseudoobstruction with morphological abnormalities of the argyrophil neurons in the myenteric plexus, associated with short small bowel, malrotation, and pyloric hypertrophy, has been previously described. We have studied a family affected by this disorder, in which the disease appeared to segregate as an X-linked recessive trait. In order to map the CIIP locus in this family, we performed linkage analysis in 26 family members by use of highly polymorphic microsatellite markers from the X chromosome. One of these markers, *DXYS154*, located in the distal part of Xq28, shows no recombination with a maximum lod score of 2.32. Multipoint analysis excluded linkage with markers spanning other regions of the X chromosome. Our results, integrated with the current genetic and physical map of Xq28, determine the order of loci as *cen-DXS15-(CIIPX)-DXS1108/DXYS154-tel*. This study establishes, for the first time, the mapping assignment of a neuropathic form of CIIP other than Hirschsprung disease.

Introduction

Chronic idiopathic intestinal pseudoobstruction (CIIP) is a clinical syndrome caused by severe abnormality of gastrointestinal motility. The patients have recurrent symptoms and signs of intestinal obstruction without any mechanical lesion. CIIP can be secondary to several diseases, such as Chagas disease, myxedema, or Duchenne muscular dystrophy (Milla 1994).

Among primary forms of CIIP are those associated with defects of enteric neuronal cells, in which anatomopathological findings include quantitative (e.g., hypo-, hyper- and a-ganglionosis) and various qualitative abnormalities (Staiano et al. 1996). In Hirschsprung disease, lack of migration of enteric ganglion cells results in a quantitative abnormality of innervation along gastrointestinal segments of variable length. In other cases, migration of enteric neurons is not affected, but enteric ganglia and nerve fibers show qualitative abnormalities, suggesting the presence of a differentiation defect.

An example of this type of defect is an inherited syndrome presenting with short small bowel, malrotation, and pyloric hypertrophy associated with morphological defects of argyrophil neurons in the myenteric plexus (Tanner et al. 1976; OMIM 243180). Genetic studies in families affected by this syndrome have been limited to clinical and anatomopathological descriptions of familiar cases, for which an autosomal recessive inheritance pattern has been proposed (Tanner et al. 1976). Here, we describe a family with a phenotype closely resembling this syndrome, showing an X-linked recessive inheritance pattern. Linkage analysis performed in this family enabled us to map the disease locus (chronic idiopathic intestinal pseudoobstruction-X chromosome; *CIIPX*) to Xq28.

Material and Methods

Clinical Features of the CIIPX Family

We have studied a patient presenting with signs and symptoms of intestinal pseudoobstruction in the first few days of life; laparotomy demonstrated a short small bowel with malrotation and pyloric hypertrophy. Histological examination of full thickness ileal and colonic biopsies, taken at 8 mo and again at 3 years, showed abnormal neurons in the myenteric plexus as well as

Received November 27, 1995; accepted for publication January 22, 1996.

Address for correspondence and reprints: Dr. Andrea Ballabio, Telethon Institute of Genetics and Medicine (TIGEM), San Raffaele Biomedical Science Park, Via Olgettina 58, 20132 Milan, Italy. E-mail: ballabio@tigem.it

0002-9297/96/5804-0011$02.00

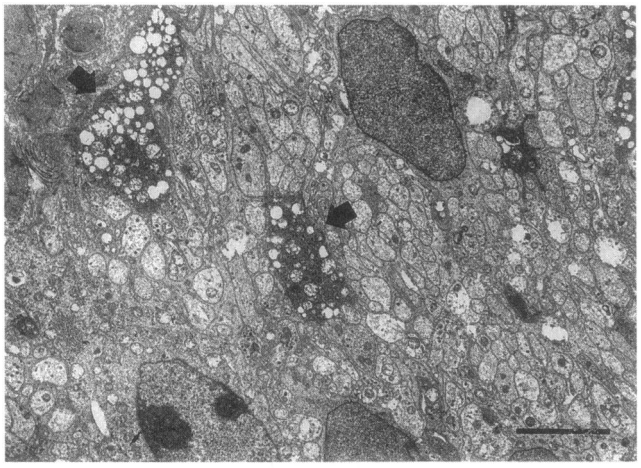

Figure 1 Electron micrograph of colonic myenteric ganglion from individual V-3, showing shrunken degenerate neurons (arrows). Scale bar 3 μm.

nerve fibers in the lamina propria in the colon (fig. 1). The clinical, morphological, and histological findings suggested that the patient was affected by an autosomal recessive syndrome described elsewhere that is characterized by intestinal pseudoobstruction due to neuronal disease, associated with a short small intestine, malrotation, and pyloric hypertrophy (Tanner et al. 1976; OMIM 243180). Therefore, the study was extended to the patient's relatives, and a condition clinically similar to the proband (fig. 2, V-3) was observed in his first cousin, V-5. Furthermore, eight additional males, related through females in the family, died in the first months after birth with gastroenterological symptoms of intestinal pseudoobstruction, suggesting an X-linked recessive inheritance of the trait (fig. 2).

Detection of Polymorphisms

Genomic DNA was isolated from whole blood by a standard procedure (Sambrook et al. 1989). In one individual, V-5, DNA was extracted from paraffin-embedded tissue. A first set of 18 primers (table 1) was selected with an average heterozygosity of 70% at an intermarker relative recombination distance of 10–20 cM (Donnelly et al. 1994; Gyapay et al. 1994; Willard et al. 1994; Genome Data Base). The second set of eleven markers was chosen in the Xq28 and Xp21.3 regions from the sources mentioned above. PCR amplification was performed following the Genome Data Base instructions. PCR products were separated on 6% acrylamide denaturing gel. Autoradiography was performed for 2–20 h.

Linkage Analysis

Simulation analysis was carried out using the SLINK and MSIM programs (Weeks et al. 1990) assuming a fully penetrant X-linked recessive model with a disease allele frequency of .0001, and a marker with four alleles with equal frequencies, corresponding to a heterozygosity of 75%. A total of 200 replicates of the pedigree were simulated under the assumption of a true recombination fraction between the disease and the marker locus of 0 and .05, respectively. To estimate false-positive rates, 2,000 replicates were simulated under the hypothesis of no linkage (true $\theta = .50$). Standard two-point and multipoint analyses were carried out using the MLINK, ILINK, and LINKMAP programs of the LINKAGE package version 5.1 (Lathrop et al. 1984) on a Sun SPARC Station IPC, on the assumption of the same parameter values for the disease gene that were used in the simulation. Equal allele frequencies ($1/n$, where n is the number of alleles) were used for each marker, since all relevant individuals were either typed, or their genotypes could be inferred from those of their relatives. Two-point and multipoint analyses including *DXYS154*, which is located in the pseudoautosomal region on the long arm of the X chromosome, were carried out as described by Ott (1986).

Results

Linkage analysis was performed on 26 available family members. Simulation analysis yielded expected and maximum lod scores of 1.67 and 2.32 for a true value of the recombination fraction between the disease and the marker locus equal to 0 and of 1.06 and 2.14 for true θ equal to .05, respectively. The probability of a false-positive result (a lod score >2, under the hypothesis of no linkage) was estimated to be 0.2% in a total of 2,000 replicates.

Following these results, we analyzed a first set of 18 markers spanning the entire X chromosome (table 1) (Donnelly et al. 1994; Gyapay et al. 1994; Willard et al. 1994). Only two markers, *DXS1214* in Xp21.3 and *DXS1108* in Xq28, gave a positive lod score of 0.30 and 1.08 at $\theta = 0$. Therefore, we decided to analyze 11 more markers from these two regions (table 1). Four additional markers from Xq28 gave positive lod scores, with a maximum of 2.32 occurring at a recombination fraction of 0 from the pseudoautosomal marker *DXYS154* (with an upper limit of the 1-lod-unit support interval corresponding to a value of $\theta = .206$). This marker was 100% informative in our pedigree (all females heterozygous). A new simulation showed that the probability of a lod score >2.3, under the hypothesis of no linkage, was only 0.05%. In contrast, all the new markers from the Xp21 region now yielded negative lod scores.

In order to exclude the possibility that the disease locus might actually be located in another region of the X chro-

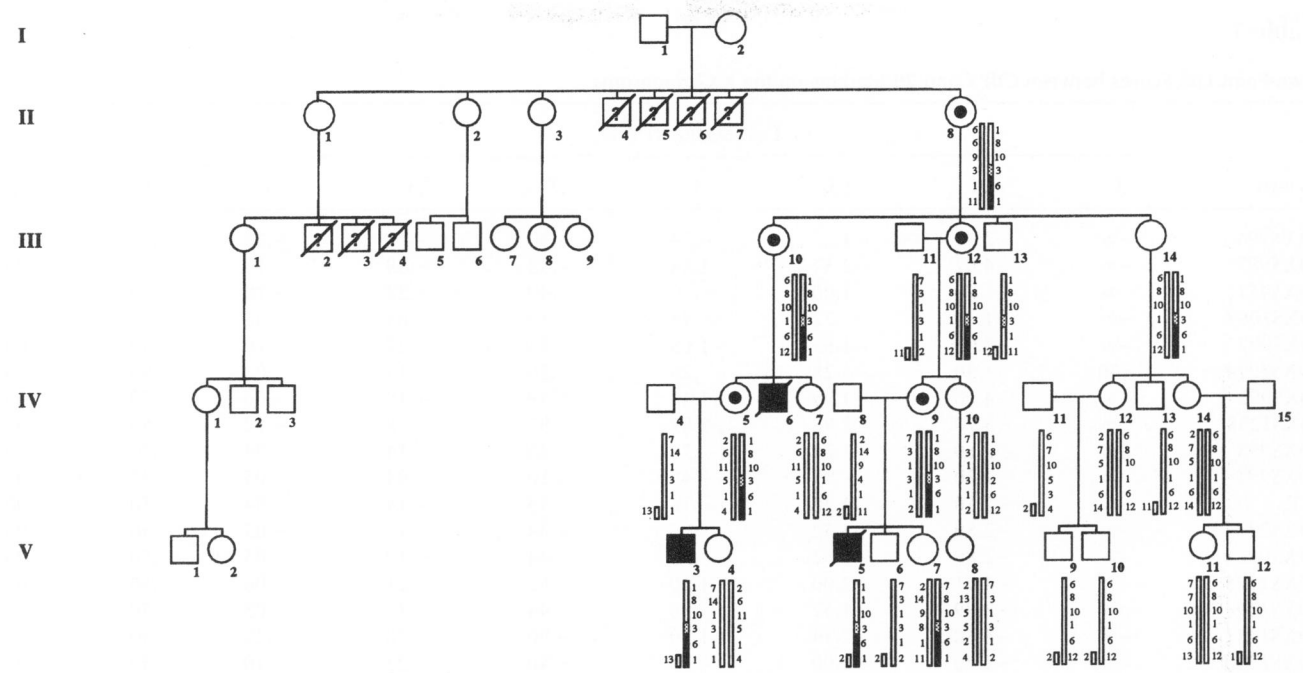

Figure 2 Complete pedigree of the CIIP family. Bars = deceased individuals; open circles containing a solid dot = obligate carriers; and question marks = individuals who died of unknown causes. Haplotypes for 6 Xq28 markers are shown for the sampled individuals (bold). Disease-associated haplotype is shown by black-filled bars. Gray-filled bars indicate that the markers in that region were not informative, and the white bars indicate the unaffected haplotype. Microsatellite markers are listed in the following order, from the top: *DXS1193, DXS52* (VNTR), *DXS15, F8C, DXS1108,* and *DXYS154.*

mosome, we carried out a series of overlapping five-point multipoint analyses (four markers plus the disease locus). All the markers included in the multipoint analyses were taken from the 1993–94 Généthon map of the X chromosome, from which information on the distances between adjacent markers was obtained (Gyapay et al. 1994). Negative lod scores were obtained in all the intervals thus tested between *DXS996* and *DXS1193,* with the only exception being the interval between *DXS984* and *DXS1200,* for which a maximum lod score of .69 was obtained (data not shown). The results of the multipoint analysis, which included six of the Xq28 markers, are shown in figure 3, *panel A.* A peak lod score of 2.32 was still obtained at 0 distance from *DXYS154,* which was already 100% informative in the two-point analysis. On the basis of analysis of recombinants, the critical region for the disease gene is therefore limited by *DXS15* toward the centromere and by the pseudoautosomal boundary toward the telomere (fig. 2).

Discussion

We report, for the first time, a family affected by an X-linked form of neuronal CIIP. Extensive histological studies performed on intestinal specimens from individual V-3 support the hypothesis that the underlying defect in this family is at the neuronal level. Deficiency of the myenteric plexus argyrophilic neurons have been described elsewhere in several cases of intestinal obstruction with malrotation, short small bowel, and pyloric hypertrophy, for which an autosomal recessive mode of inheritance has been proposed (Tanner et al. 1976). A similar phenotype is present in our family, suggesting that this clinical entity can be associated with different loci.

To begin studying this developmental disorder at the molecular level, we localized the gene for X-linked neuronal CIIP to Xq28. The significant lod score obtained with *DXYS154,* compared to the negative ones for the other microsatellites mapping to regions other than Xq28, strongly supports the localization of the CIIP gene to this area. The penetrance of the disease in this family appears to be complete. None of the unaffected sons of obligate carriers manifests any symptoms of CIIP. Although intestinal histological data are not available, we presume that these asymptomatic males do not carry the disease gene, since all males manifesting the disease, except individual V-3, died with acute symptoms of bowel obstruction within the first months after birth. Data from the 1994 X Chromosome Workshop assigns the order of loci as *cen-DXS1193-DXS52-DXS15-DXS1177-DXS1108-DXYS154-tel* in Xq28 (Willard et al. 1994). The critical region is defined by marker

Table 1

Two-Point Lod Scores between CIIPX and 29 Markers on the X Chromosome

	Lod Score at θ =								
Locus	.0	.01	.05	.1	.2	.3	.4	$\hat{\theta}$	Z_{max}
DXS996	−∞	−2.60	−1.27	−.74	−.30	−.11	−.02	.50	.00
DXS987	−∞	−4.62	−2.54	−1.66	−.82	−.38	−.13	.50	.00
DXS451	−∞	−1.70	−1.00	−.70	−.40	−.22	−.10	.50	.00
DXS1067	−∞	−1.40	−.72	−.44	−.19	−.08	−.02	.50	.00
DXS997	−∞	−3.03	−1.65	−1.08	−.54	−.27	−.10	.50	.00
DXS1214	.30	.30	.28	.26	.20	.15	.08	.00	.30
DXS992	−∞	−4.00	−1.99	−1.19	−.49	−.19	−.04	.50	.00
DXS1238	−∞	−5.70	−2.98	−1.87	−.87	−.38	−.12	.50	.00
DXS993	−∞	−2.60	−1.28	−.76	−.33	−.14	−.04	.50	.00
DXS991	−∞	−2.30	−.99	−.49	−.10	.04	.05	.37	.06
AR	−∞	−2.60	−1.28	−.76	−.33	−.14	−.04	.50	.00
DXS227	−∞	−2.89	−1.52	−.96	−.44	−.19	−.05	.50	.00
DXS986	−∞	−2.89	−1.52	−.96	−.44	−.19	−.05	.50	.00
DXS1225	−∞	−4.01	−2.00	−1.20	−.52	−.21	−.06	.50	.00
DXS1196	−∞	−2.89	−1.52	−.96	−.44	−.19	−.05	.50	.00
DXS1231	−∞	−4.60	−2.54	−1.70	−.90	−.48	−.20	.50	.00
DXS1210	−∞	−1.70	−1.00	−.70	−.40	−.22	−.10	.50	.00
DXS424	−∞	−.61	.00	.19	.28	.23	.14	.20	.28
DXS1047	−∞	−4.30	−2.27	−1.45	−.73	−.39	−.20	.50	.00
DXS984	−∞	−1.04	−.40	−.17	−.01	.02	.02	.32	.02
DXS1200	−∞	−.31	.30	.48	.53	.44	.25	.17	.54
DXS1215	−∞	−.93	−.29	−.07	.09	.11	.08	.28	.12
DXS1193	−∞	−.02	.52	.64	.61	.46	.25	.13	.65
DXS52	−∞	−1.20	−.47	−.15	.10	.17	.13	.30	.17
DXS15	−∞	−1.15	−.34	−.00	.26	.29	.20	.27	.30
DXS1177	1.59	1.57	1.47	1.35	1.07	.76	.41	.00	1.59
F8C	1.11	1.09	1.02	.93	.73	.51	.27	.00	1.11
DXS1108	1.08	1.07	1.02	.93	.74	.51	.26	.00	1.08
DXYS154	2.32	2.27	2.08	1.83	1.35	.89	.44	.00	2.32

Note.—Markers are listed from the Xp telomere to the Xq telomere. Markers used in the first part of the analysis are in italics. Markers chosen for the second part of the analysis are in bold.

DXS15, showing no recombination with CIIP and the pseudoautosomal boundary. This region spans 4.4 cM, corresponding to 3 Mb on the physical map.

Several genes have been identified in the Xq28 region, and most of them appear to be clustered in the 2 Mb of DNA between the *G6PD* and *DXS15* loci, where the *CIIPX* critical region is located (Maestrini et al. 1992; Bione et al. 1993; Sedlacek et al. 1993). Some of these genes may be considered good candidates for an involvement in CIIP, on the basis of the type of protein they encode and their expression pattern (fig. 3, *panel B*). The filamin gene (ABP-280), for example, encodes a protein that links actin filaments to membrane glycoproteins and can play an important role in the cytoskeletal organization of neurons (Gorlin et al. 1993). Another candidate gene is the human homologue of bovine *rab* GDI (XAP 4) (Sedlacek et al. 1993), which was initially identified as an inhibitory GDP/GTP exchange for *rab* 3A, a protein implicated in neurotransmitter release. The gene is expressed in several rat tissues, including the small intestine (Matsui et al. 1990), and appears to be involved in the regulation of intracellular vesicle traffic (Araki et al. 1990; Shirataki et al. 1993).

Migration and differentiation of enteric neuronal cells from the neural crest during the first weeks of development is a complex process in which several genes encoding for membrane receptors, their ligands, intracellular signaling substrates, transcription factors, and extracellular matrix components play a major role. This is underlined by the involvement of the RET protooncogene (Edery et al. 1994; Mulligan et al. 1994; Romeo et al. 1994; Angrist et al. 1995*a,* 1995*b*) and, more recently, of the gene encoding the endothelin-B receptor (EDNRB) (Puffenberger et al. 1994; Attie' et al. 1995*b*), in the pathogenesis of Hirschsprung disease, the most common form of neuronal intestinal pseudoobstruction. It is interesting to note that higher penetrance of HSCR in males compared to females (Badner et al. 1990) was

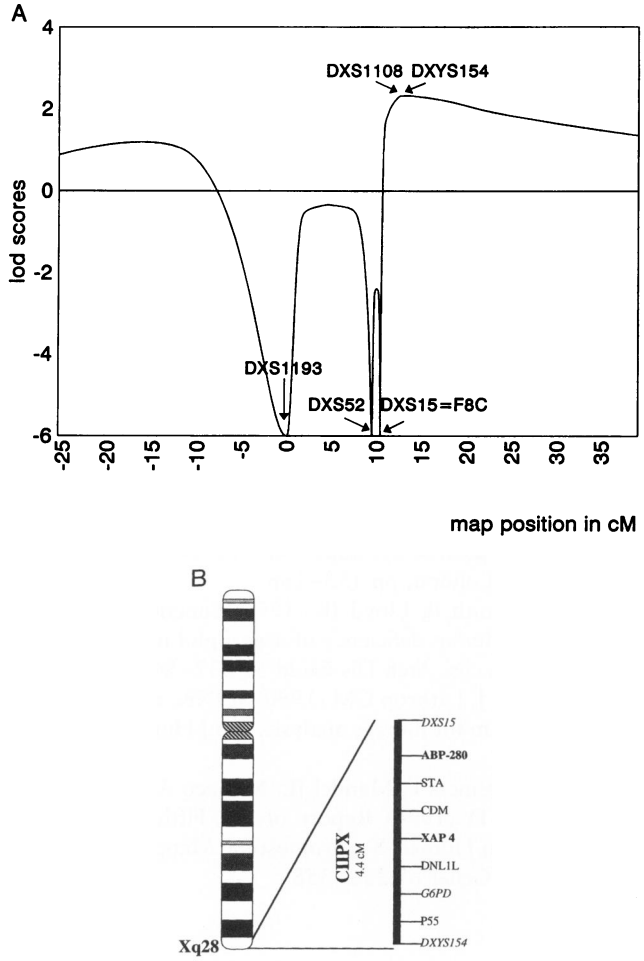

Figure 3 *A*, Multipoint linkage map of *CIIPX* and Xq28. Marker *DXS1193* was chosen arbitrarily as the origin for the map. Intermarker distances were taken from references mentioned in the text. Recombination fractions were converted into centimorgans by using Haldane's map function. *B*, Schematic representation of *CIIPX* critical region, including some of the genes mapping in the interval. Flanking markers are in italic. Candidate genes are in bold. ABP-280 is the filamin gene (Gorlin et al. 1993). STA is the gene mutated in Emery-Dreyfuss muscular dystrophy (Bione et al. 1994). CDM is a gene with similarity to the rod-like tail portion of heavy-chain myosins (Mosser et al. 1994). XAP 4 is the human homologue of the bovine rab GDI (Sedlacek et al. 1993). DNL1L is homologue to Dnase I (Parrish et al. 1995). p55 encodes for a palmitoylated membrane protein (Metzenberg and Gitschier 1992).

observed in both RET and EDNRB mutations (Puffenberger et al. 1994; Attie' et al. 1995*a*). An intriguing hypothesis might be that *CIIPX* represents an additional susceptibility locus in Hirschsprung disease.

Acknowledgments

We thank Dr. S. Cucchiara for providing clinical information and helpful suggestions and Dr. Gambini for supplying patient V-5 paraffin-embedded tissue. This work was supported by the Italian Telethon Foundation and by National Institutes of Health grant HG00008 (to M.D.). V.B. is recipient of an Italian Telethon fellowship.

References

Angrist M, Bolk S, Thiel B, Puffenberger EG, Hofstra RM, Buys CHCM, Cass DT, et al (1995) Mutation analysis of the RET receptor tryrosine kinase in Hirschsprung disease. Hum Mol Genet 4:821–830

Araki S, Kikuchi A, Hata Y, Isomura M, Takai Y (1990) J Biol Chem 265:13007–13015

Attie' T, Pelet A, Edery P, Eng C, Mulligan LM, Amiel J, Boutrand L, et al (1995*a*) Diversity of the RET proto-oncogene mutations in familial and sporadic Hirschsprung disease. Hum Mol Genet 4:1381–1386

Attie' T, Till M, Amiel J, Edery P, Boutrand L, Munnich A, Lyonnet S (1995*b*) Mutation of the Endothelin-receptor B gene in Waardenburg-Hirschsprung disease. Hum Mol Genet 4:2407–2409

Badner JA, Sieber WK, Garver KL, Chakravarti A (1990) A genetic study of Hirschsprung disease. Am J Hum Genet 46:568–580

Bione S, Maestrini E, Rivella S, Mancini M, Regis S, Romeo G, Toniolo D (1994) Identification of a novel X-linked gene responsible for Emery-Dreifuss muscular dystrophy. Nat Genet 8:323–327

Bione S, Tamanini F, Maestrini E, Tribioli C, Poustka A, Torri G, Rivella S, et al (1993) Transcriptional organization of a 450-kb region of the human X chromosome in Xq28. Proc Natl Acad Sci USA 90:10977–10981

Donnelly A, Kozman H, Gedeon AK, Webb S, Lynch M, Sutherland GR, Richards RI, et al (1994) A linkage map of microsatellite markers on the human X chromosome. Genomics 20:363–370

Edery P, Lyonnet S, Mullingan LM, Pelet A, Dow E, Abel L, Holder S, et al (1994) Mutations of the *RET* proto-oncogene in Hirschsprung's disease. Nature 367:378–380

Fain PR, Kort EN, Chance PF, Nguyen K, Redd DF, Econs MJ, Barker DF (1995) A 2D crossover-based map of the human X chromosome as a model for map integration. Nat Genet 9:261–266

Freije D, Helms C, Watson MS, Donis-Keller H (1992) Identification of a second pseudoautosomal region near the Xq and Yq telomeres. Science 258:1784–1787

Gorlin JB, Henske E, Warren ST, Kunst CB, D'Urso M, Palmieri G, Hartwig JH, et al (1993) Actin-binding protein (ABP-280) filamin gene (FLN) maps telomeric to the color vision locus (R/GCP) and centromeric to G6PD in Xq28. Genomics 17:496–498

Gyapay G, Morissette J, Vignal A, Dib C, Fizames C, Millasseau P, Marc S, et al (1994) The 1993–94 Généthon human genetic linkage map. Nat Genet 7:246–339

Lathrop GM, Lalouel JM, Julier C, Ott J (1984) Strategies for multilocus linkage analysis in humans. Proc Natl Acad Sci USA 81:3443–3446

Maestrini E, Tamanini F, Kioschis P, Gimbo E, Marinelli P,

Tribioli C, D'Urso M, et al (1992) An archipelago of CpG islands in Xq28: identification and fine mapping of 20 new CpG islands of the human X chromosome. Hum Mol Genet 1:275–280

Matsui Y, Kikuchi A, Araki S, Hata Y, Kondo J, Teranishi Y, Takai Y (1990) Mol Cell Biol 10:4116–4122

Metzenberg AB, Gitschier J (1992) The gene encoding the palmitoylated erythrocyte membrane protein, p55, originates at the CpG island 3′ to the factor VIII gene. Hum Mol Genet 1:97–101

Milla PJ (1994) Intestinal pseudo-obstruction in children. In: Kamm MA, Lennard-Jones JE (eds) Constipation. Wrightson Biomedical, Petersfield, UK, and Bristol, PA, pp 251–257

Mosser J, Sarde C-O, Vicaire S, Yates JRW, Mandel J-L (1994) A new human gene (DXS1357E) with ubiquitous expression, located in Xq28 adjacent to the adrenoleukodystrophy gene. Genomics 22:469–471

Mulligan LM, Eng C, Attie T, Lyonnet S, Marsh DJ, Hyland VJ, Robinson BG, et al (1994) Diverse phenotypes associated with exon 10 mutations of the *RET* proto-oncogene. Hum Mol Genet 3:2163–2167

Ott J (1986) Y-linkage and pseudoautosomal linkage. Ame J Hum Genet 38:891–897

Parrish JE, Ciccodicola A, Wehnert M, Cox GF, Chen E, Nelson DL (1995) A muscle-specific DNase I-like gene in human Xq28. Hum Mol Genet 4:1557–1564

Puffenberger EG, Hosoda K, Washington SS, Nakao K, deWit D, Yanagisawa M, Chakravarti A (1994) A missense mutation of the endothelin-B receptor gene in multigenic Hirschsprung's disease. Cell 79:1257–1266

Romeo G, Ronchetto P, Luo Y, Barone V, Serl M, Ceccherini I, Pasini B, et al (1994) Point mutations affecting the tyrosine kinase domain of the *RET* proto-oncogene in Hirschsprung's disease. Nature 367:377–378

Sambrook J, Fritsch EF, Maniatis T (1989) Molecular cloning: a laboratory manual, 2d ed. Cold Spring Harbor Laboratory Press, Cold Spring Harbor, NY

Sedlacek Z, Korn B, Konecki DS, Siebenhaar R, Coy JF, Kioschis P, Poustka A (1993) Construction of a transcription map of a 300 kb region around the human G6PD locus by direct cDNA selection. Hum Mol Genet 2:1865–1869

Shirataki H, Kaibuchi K, Sakoda T, Kishida S, Yamaguchi T, Wada K, Miyazaki M, et al (1993) Rabphilin-3A, a putative target protein for smg p25a/rab3A p25 small GTP-binding protein, related to synaptogamin. Mol Cell Biol 13:2061–2068

Staiano A, Tozzi A, Auricchio A (1996) Aetiology and assessment of constipation in children. In: Bailler-Tindall (ed) Baillier's clinical gastroenterology—chronic constipation. Baillier-Tindall, London, pp 153–168

Tanner MS, Smith B, Lloyd JK (1976) Functional intestinal obstruction due to deficiency of argyrophil neurones in the myenteric plexus. Arch Dis Child 51:837–841

Weeks DE, Ott J, Lathrop GM (1990) SLINK: a general simulation program for linkage analysis. Am J Hum Genet Suppl 47:A204

Willard HF, Cremers F, Mandel JL, Monaco AP, Nelson DL, Schlessinger D (1994) Report of the Fifth International Workshop on Human X Chromosome Mapping 1994. Cytogenet Cell Genet 67:296–358